Effect of amorphous Si capping layer on the hole transport properties of BaSi2 and improved conversion efficiency approaching 10% in p-BaSi2/n-Si solar cells

Suguru Yachi, Ryota Takabe, Hiroki Takeuchi, Kaoru Toko, and Takashi Suemasu

---

Articles you may be interested in

Influence of air exposure duration and a-Si capping layer thickness on the performance of p-BaSi2/n-Si heterojunction solar cells
AIP Advances **6**, 085107 (2016); 10.1063/1.4961063

p-BaSi2/n-Si heterojunction solar cells with conversion efficiency reaching 9.0%
Appl. Phys. Lett. **108**, 152101 (2016); 10.1063/1.4945725

Reduction of Cu-rich interfacial layer and improvement of bulk CuO property through two-step sputtering for p-CuO/n-Si heterojunction solar cell
J. Appl. Phys. **116**, 074501 (2014); 10.1063/1.4893321

In-situ heavily p-type doping of over 1020 cm−3 in semiconducting BaSi2 thin films for solar cells applications
Appl. Phys. Lett. **102**, 112107 (2013); 10.1063/1.4796142

Improved photoresponsivity of semiconducting BaSi2 epitaxial films grown on a tunnel junction for thin-film solar cells
Appl. Phys. Lett. **100**, 152114 (2012); 10.1063/1.3703585

Effect of amorphous Si capping layer on the hole transport properties of BaSi$_2$ and improved conversion efficiency approaching 10% in p-BaSi$_2$/n-Si solar cells

Suguru Yachi, Ryota Takabe, Hiroki Takeuchi, Kaoru Toko, and Takashi Suemasu

Institute of Applied Physics, University of Tsukuba, Tsukuba, Ibaraki 305-8573, Japan

We investigated the effect of a 3-nm-thick amorphous Si (a-Si) capping layer on the hole transport properties of BaSi$_2$ films. The contact resistance decreased with decreasing resistivity of p-BaSi$_2$ and reached a minimum of 0.35 $\Omega \cdot$cm^2. The effect of the a-Si layer was confirmed by higher photoresponsivities for n-BaSi$_2$ films capped with the a-Si layer than for those without the a-Si layer, showing that the minority carriers (holes) were extracted efficiently across the a-Si/n-BaSi$_2$ interface. Under AM1.5 illumination, the conversion efficiency reached 9.9% in a-Si(3 nm)/p-BaSi$_2$(20 nm)/n-Si solar cells, the highest value ever reported for semiconducting silicides. *Published by AIP Publishing.*
[http://dx.doi.org/10.1063/1.4961309]

Extensive research has been carried out on numerous solar cell materials other than silicon, such as chalcopyrite, cadmium telluride, and perovskite, to realize higher efficiency solar cells with lower cost. However, these materials contain scarce and/or toxic elements. Thus, the exploration of alternative materials is very important. Among such materials, we have paid special attention to semiconducting BaSi$_2$,[1–3] which is composed of earth-abundant elements. It has a bandgap of 1.3 eV,[4,5] matching the solar spectrum. One of the most attractive features of this material is that a large absorption coefficient α,[5–7] comparable to those of Cu(In,Ga)Se$_2$, and a large minority-carrier lifetime $\tau \approx 10\,\mu$s,[8,9] giving a large minority-carrier diffusion length $L \approx 10\,\mu$m,[10] can be utilized. An energy conversion efficiency η of over 25% can be expected for a 2-μm-thick BaSi$_2$ pn junction diode.[11] For device application, surface passivation is very important for materials like BaSi$_2$ which have large α. This is because the short-wavelength light is absorbed in the region close to the surface. Hence, a defective surface deteriorates the solar cell performance. Microwave-detected photoconductivity decay measurements reveal that an a-Si capping layer ensures τ can reach approximately 10 μs with an excellent repeatability for intrinsically doped n-BaSi$_2$.[12] Intrinsically doped BaSi$_2$ shows n-type conductivity, with an electron concentration n on the order of 10^{16} cm^{-3}.[4,13] A first-principles density functional theory supercell approach revealed that this n-type conductivity arises from Si vacancies.[14] Hereafter, we denote intrinsically doped n-BaSi$_2$ simply as n-BaSi$_2$. As a next step, a deep understanding of the carrier transport properties across the a-Si/BaSi$_2$ heterointerface is very important. For the a-Si/n-BaSi$_2$ interface, we found from hard X-ray photoelectron spectroscopy (HAXPES) that the barrier height of the a-Si for the minority-carriers, holes, in the n-BaSi$_2$ is -0.2 eV,[15] meaning that the transport of holes across the interface is not blocked, whereas this value is approximately 3.9 eV at the native oxide/n-BaSi$_2$ interface.[16] It was also found that the oxidation of BaSi$_2$ is suppressed significantly by the a-Si capping layer. The alignment of the valence-band maximums

of BaSi$_2$ ($E_V^{\mathrm{BaSi_2}}$), its native oxide (E_V^{oxide}), and a-Si ($E_V^{\mathrm{a-Si}}$) is schematically shown in Fig. 1. Because of the a-Si capping layer, we recently achieved $\eta = 9.0\%$ in p-BaSi$_2$/n-Si solar cells.[17] However, we have only limited information about the hole transport properties across the a-Si/p-BaSi$_2$ interface.

In this study, we aim to investigate the hole transport properties across the a-Si/BaSi$_2$ interface. We first evaluated the effect of a-Si capping layer on the contact resistance of boron (B)-doped p-BaSi$_2$. Contact resistance R_C is one of the most important parameters that directly affects the fill factor (FF), thereby leading to the reduction of η. Many studies have been conducted about R_C for solar cell materials.[18–24] However, there have been no reports on BaSi$_2$. Coaxial impact-collision ion scattering spectroscopy revealed that the surface of an *a*-axis-oriented BaSi$_2$ epitaxial film is terminated by Si tetrahedra.[25] We next investigated its effect on
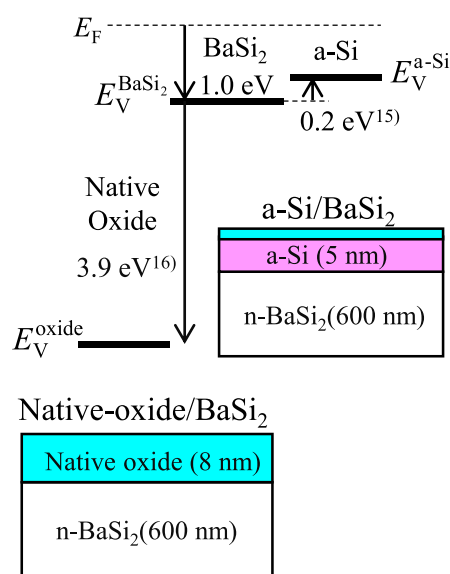

FIG. 1. The alignment of valence-band maximums of BaSi$_2$ ($E_V^{\mathrm{BaSi_2}}$), its native oxide (E_V^{oxide}), and a-Si ($E_V^{\mathrm{a-Si}}$).[15,16] Sample structures used for HAXPES measurements are schematically shown.

the transport of photogenerated holes in n-BaSi$_2$ across the a-Si/n-BaSi$_2$ interface, and finally checked it using p-BaSi$_2$/n-Si solar cells, where we achieved the highest value of $\eta = 9.9\%$ under AM1.5 illumination.

A molecular beam epitaxy (MBE) system (R-DEC Co., Ltd.) equipped with an electron-beam evaporation source for Si and standard Knudsen cells (K-cell) for Ba and B was used in this investigation. Details of the growth procedure of n-BaSi$_2$ and B-doped p-BaSi$_2$ have been reported previously.[26,27] For R_C measurements, we used high-resistivity floating-zone n-Si(111) substrates (resistivity $\rho > 1000$ Ω cm) to avoid current flowing via the substrate. 250-nm-thick n-BaSi$_2$ and 500-nm-thick B-doped p-BaSi$_2$ layers were epitaxially grown by MBE, followed by *in situ* 5-nm-thick a-Si capping layers deposited at a substrate temperature $T_S = 180\,°C$. The hole concentration p, measured by the van der Pauw method, was varied from 5.7×10^{17} cm^{-3} to 5.0×10^{18} cm^{-3} by changing the temperature of the B K-cell crucible from $1170\,°C$ to $1350\,°C$. After that, 200-nm-thick stripe-shaped Al or ITO electrodes with dimensions of 7×0.6 mm^2 were formed by sputtering at an interval of 1 mm. Contact resistance was measured by the transfer length method (TLM).[28]

To determine the photoresponse properties, a 500-nm-thick n-BaSi$_2$ layer was epitaxially grown on Czochralski n-Si(111) ($\rho < 0.01$ Ω cm), and a 3-nm-thick a-Si capping layer was deposited at $T_S = 180\,°C$. Regarding the a-Si layer thickness, it was found from recent experiments that 5-nm-thick a-Si induces absorption loss, especially in the wavelength range below approximately 730 nm, which is equivalent to the bandgap energy of a-Si. That is why we adopted 3 nm as the a-Si layer thickness. Next, 200-nm-thick ITO surface electrodes with diameters of 1 mm and Al rear electrodes were fabricated by sputtering. Photoresponse and reflectance (R) spectra were evaluated at room temperature by a lock-in technique using a xenon lamp with a 25-cm-focal-length single monochromator (Bunko Keiki SM-1700A and RU-60N). The light intensity was calibrated using a pyroelectric sensor (Melles Griot 13PEM001/J). Finally, we formed a 20-nm-thick B-doped p-BaSi$_2$ layer on CZ-n-Si(111) ($\rho = 1$–4 Ω cm), followed by a 3-nm-thick a-Si capping layer; 80-nm-thick ITO surface electrodes with diameters of 1 mm and Al rear electrodes were fabricated by sputtering. The hole concentration p was set to approximately 2.0×10^{18} cm^{-3}. In this device structure, photogenerated carriers are expected to separate efficiently because of the large conduction-band offset (0.9 eV) and valence-band offset (0.7 eV) at the p-BaSi$_2$/n-Si interface.[17] For comparison, a p-BaSi$_2$/n-Si solar cell without the a-Si capping layer was also formed. Current density versus voltage (J-V) curves were measured under standard AM1.5, 100 mW/cm^2 illumination at approximately $25\,°C$. For all the samples, epitaxial growth of BaSi$_2$ layers was confirmed by reflection high-energy electron diffraction and θ-2θ x-ray diffraction.

Figure 2(a) shows examples of the relationship between resistance and electrode distance for ITO electrodes on n-BaSi$_2$ ($n = 3.6 \times 10^{16}$ cm^{-3}) and p-BaSi$_2$ ($p = 5.7 \times 10^{17}$ cm^{-3}). The resistance increases almost linearly with electrode distance for all the samples. The linear extrapolation to the vertical line gives $2 \times R_C$. The R_C was drastically

decreased by capping with the a-Si layer, as shown in Fig. 2(b). This is because the a-Si layer prevents surface oxidation of the BaSi$_2$ layers.[15] It was found from our previous study that the native oxide layer thickness is approximately 8 nm.[16] This native oxide layer disturbs the current flow and leads to an increase in R_C.

We next focus on the transport of majority carriers (holes) of p-BaSi$_2$ across the a-Si/p-BaSi$_2$ interface and then move on to the transport of photogenerated minority carriers (holes) of n-BaSi$_2$ across the a-Si/n-BaSi$_2$ interface. Figure 3 shows the relationship between R_C and resistivity for p-BaSi$_2$. There is a tendency for R_C to decrease as the resistivity decreases. The R_C reached a minimum of 0.35 Ω cm^2 for Al/p-BaSi$_2$ when p was 4.0×10^{18} cm^{-3}. In Ref. 28, the dependence of R_C on the sheet resistance is given by

$$R_C = R_{sheet} \times L_t^2, \tag{1}$$

where R_{sheet} is the sheet resistance and L_t is the transfer length. R_{sheet} is proportional to the resistivity. Therefore, the decrease in resistivity causes a decrease in R_{sheet}, leading to
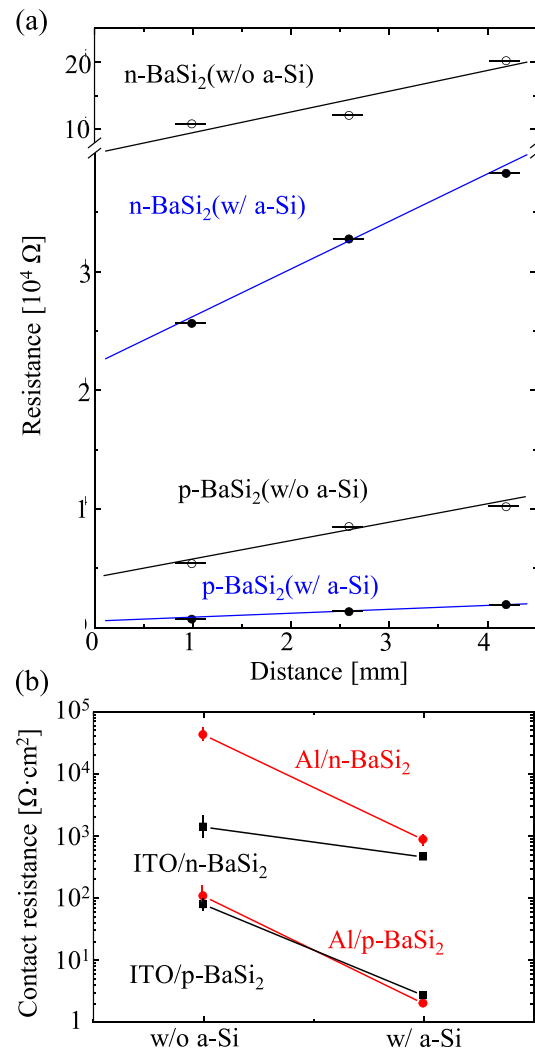

FIG. 2. (a) Relationship between resistance and electrode distance for n-BaSi$_2$ ($n = 3.6 \times 10^{16}$ cm^{-3}, 250 nm) and B-doped p-BaSi$_2$ ($p = 5.7 \times 10^{17}$ cm^{-3}, 500 nm) capped with or without a 5-nm-thick a-Si layer. (b) Effect of the a-Si capping layer on R_C in BaSi$_2$.
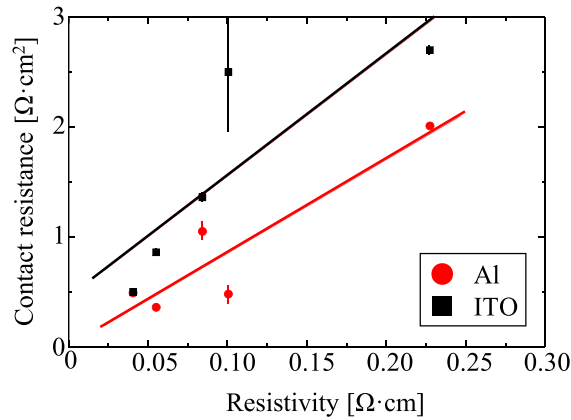
FIG. 3. Dependence of R_C on resistivity of B-doped p-BaSi$_2$ (500 nm) using Al or ITO electrodes. p was varied in a range between 5.7×10^{17} cm^{-3} and 5.0×10^{18} cm^{-3}.

a decrease in R_C. The result shown in Fig. 3 is consistent with Eq. (1).

Figures 4(a) and 4(b) show the photoresponse and reflectance spectra of 500-nm-thick n-BaSi$_2$ capped without or with the a-Si layer, respectively. The bias voltages were applied so that the photogenerated holes in the n-BaSi$_2$ were transferred to the surface electrode (ITO) across the a-Si/n-BaSi$_2$ interface. The reflectance was almost the same for both samples, regardless of the a-Si capping layer. Hence, the influence of the a-Si on R is negligible; therefore, the number of photogenerated carriers should be almost the same. The photoresponsivity was drastically improved, by
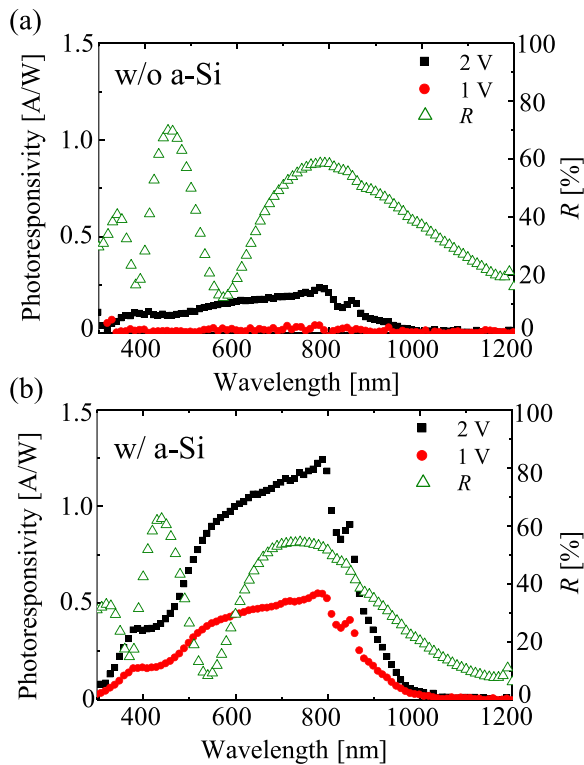
approximately five times, for BaSi$_2$ capped with the a-Si layer compared with that without the a-Si layer. This distinct difference is ascribed to the difference in hole transport properties between a-Si/n-BaSi$_2$ and native-oxide/n-BaSi$_2$ interfaces; hole transport in n-BaSi$_2$ is not blocked across the a-Si/n-BaSi$_2$ interface, whereas it is blocked at the native-oxide/n-BaSi$_2$ interface. The results presented in Fig. 4 are consistent with the band lineups shown in Fig. 1, obtained by HAXPES.

Figure 5(a) shows the *J-V* characteristics under AM1.5 illumination for the p-BaSi$_2$($p = 2.0 \times 10^{18}$ cm^{-3}, 20 nm)/n-Si solar cell with or without the a-Si capping layer. The sample capped with the a-Si layer shows $\eta = 9.9\%$, a short-circuit current density J_{SC} of 35.2 mA/cm^2, and an open-circuit voltage V_{OC} of 0.47 V. This efficiency is the largest ever reported for
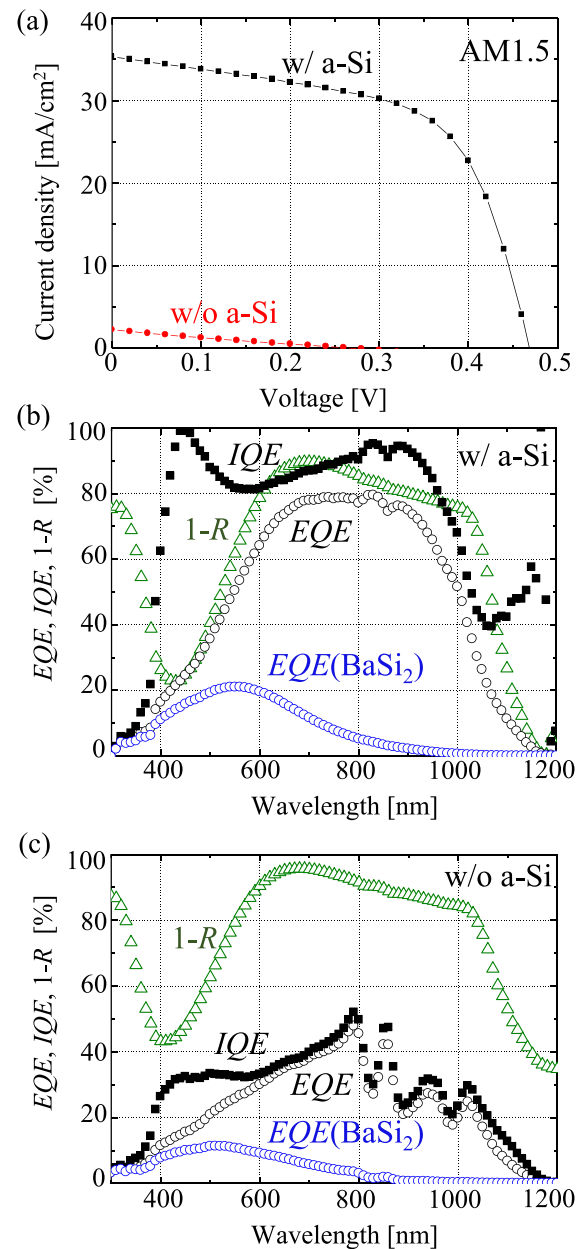

FIG. 4. Photoresponse and reflectance spectra of n-BaSi$_2$ (500 nm) (a) without and (b) with a 3-nm-thick a-Si capping layer. The bias voltages were applied so that the photogenerated minority carriers (holes) in the n-BaSi$_2$ were transferred to the surface electrode (ITO) across the a-Si/n-BaSi$_2$ interface.

FIG. 5. (a) *J-V* characteristics of p-BaSi$_2$ ($p = 2.0 \times 10^{18}$ cm^{-3}, 20 nm)/n-Si solar cells with or without the a-Si capping layer under AM1.5 illumination; (b) *EQE*, *EQE*(BaSi$_2$), *IQE*, and 1-*R* spectra for sample capped with the a-Si layer; and (c) those for sample without the a-Si layer.

TABLE I. Solar cell properties are specified.

Structure	J_{SC} (mA/cm^2)	V_{OC} (V)	FF	η (%)	R_S (Ω)	R_{SH} (Ω)	γ	J_0 (mA/cm^2)
w/ a-Si	35.2	0.47	0.60	9.9	128	10046	1.17	1.49×10^{-5}
w/o a-Si	2.24	0.27	0.22	0.1	392	4376	1.33	1.21×10^{-6}

solar cells using semiconducting silicides. In contrast, the sample without the a-Si capping layer showed a very small η of only 0.1%. Solar cell parameters such as series resistance R_S were derived using the following equation:[29]

$$\frac{dV}{dJ} = SR_S + \frac{\gamma k_B T}{q} \left[\frac{1 - (SR_{SH})^{-1} dV/dJ}{J + J_{SC} - (SR_{SH})^{-1} V} \right], \quad (2)$$

where J_0 is the reverse-bias saturation current density, S is the device area, R_{SH} is the shunt resistance, and γ is the diode ideality factor. Parameters including FF are shown in Table I. Almost all parameters were improved by the a-Si capping layer. Figures 5(b) and 5(c) show the external quantum efficiency (EQE), internal quantum efficiency (IQE), and 1-R spectra for samples capped with or without the a-Si layer, respectively. The contribution of BaSi$_2$ to EQE is given by EQE(BaSi$_2$). There is no much difference in 1-R spectra between the two samples, whereas the values of EQE, EQE(BaSi$_2$), and IQE differ so much, demonstrating the impact of the a-Si capping layer on the solar cell performance. The small V_{OC} (0.47 V) is caused by a small built-in potential of approximately 0.1 V, whereby photogenerated carriers are not separated by the electrostatic field around the pn junction but by the large band offset at the heterointerface. Once photogenerated electrons are accumulated in the n-Si, for example, the Fermi level E_F of the n-Si goes up with respect to the E_F of the p-BaSi$_2$, giving rise to the band bending in the n-Si. This band bending acts to prevent the transport of minority carriers (holes) in the n-Si toward the p-BaSi$_2$ across the interface. The same thing occurs in the p-BaSi$_2$ region. Another cause might be the defects at the heterointerface arising from the difference in crystal structure between Si and BaSi$_2$. In this sense, a classic homojunction diode is necessary to improve the V_{OC}. On the basis of these results, we conclude that the capping of p-BaSi$_2$ with a-Si layers is a very effective means to ensure good hole transport across the a-Si/p-BaSi$_2$ interface, together with surface passivation with sufficiently large τ for thin-film solar cell applications.

In summary, we examined the effect of an a-Si capping layer on the carrier transport properties of n-BaSi$_2$ and B-doped p-BaSi$_2$ layers grown by MBE. The R_C significantly decreased with the a-Si capping layer for both n-BaSi$_2$ and p-BaSi$_2$ layers and reached a minimum of 0.35 Ω cm^2 for Al/ p-BaSi$_2$ at $p = 4.0 \times 10^{18}$ cm^{-3}. The effect of the a-Si capping layer was also confirmed by the transport of minority carriers (holes) photogenerated in n-BaSi$_2$ across the a-Si/ n-BaSi$_2$ interface. The photoresponsivity of n-BaSi$_2$ was

improved drastically, by a factor of five, by the a-Si capping layer. Finally, we achieved $\eta = 9.9\%$ in p-BaSi$_2$(20 nm)/n-Si solar cells. This study demonstrates the impact of the a-Si capping layer on the carrier transport properties of BaSi$_2$.

[1] H. K. Janzon, H. Schäfer, and A. Weiss, Z. Anorg. Allg. Chem. **372**, 87 (1970).
[2] J. Evers, G. Oehlinger, and A. Weiss, Angew. Chem., Int. Ed. **16**, 659 (1977).
[3] M. Imai and T. Hirano, J. Alloys Compd. **224**, 111 (1995).
[4] K. Morita, Y. Inomata, and T. Suemasu, Thin Solid Films **508**, 363 (2006).
[5] K. Toh, T. Saito, and T. Suemasu, Jpn. J. Appl. Phys., Part 1 **50**, 068001 (2011).
[6] D. B. Migas, V. L. Shaposhnikov, and V. E. Borisenko, Phys. Status Solidi B **244**, 2611 (2007).
[7] M. Kumar, N. Umezawa, and M. Imai, J. Appl. Phys. **115**, 203718 (2014).
[8] K. O. Hara, N. Usami, K. Toh, M. Baba, K. Toko, and T. Suemasu, J. Appl. Phys. **112**, 083108 (2012).
[9] K. O. Hara, N. Usami, K. Nakamura, R. Takabe, M. Baba, K. Toko, and T. Suemasu, Appl. Phys. Express **6**, 112302 (2013).
[10] M. Baba, K. Toh, K. Toko, N. Saito, N. Yoshizawa, K. Jiptner, T. Sakiguchi, K. O. Hara, N. Usami, and T. Suemasu, J. Cryst. Growth **348**, 75 (2012).
[11] T. Sueamsu, Jpn. J. Appl. Phys., Part 1 **54**, 07JA01 (2015).
[12] R. Takabe, K. O. Hara, M. Baba, W. Du, N. Shimada, K. Toko, N. Usami, and T. Suemasu, J. Appl. Phys. **115**, 193510 (2014).
[13] W. Du, M. Baba, K. Toko, K. O. Hara, K. Watanabe, T. Sekiguchi, N. Usami, and T. Suemasu, J. Appl. Phys. **115**, 223701 (2014).
[14] M. Kumar, N. Umezawa, and M. Imai, in 63rd Japan Society of Applied Physics Spring Meeting, 21a-S223-2, Tokyo, March 21, 2016.
[15] R. Takabe, H. Takeuchi, W. Du, K. Ito, K. Toko, S. Ueda, A. Kimura, and T. Suemasu, J. Appl. Phys. **119**, 165304 (2016).
[16] R. Takabe, W. Du, K. Ito, H. Takeuchi, K. Toko, S. Ueda, A. Kimura, and T. Suemas, J. Appl. Phys. **119**, 025306 (2016).
[17] D. Tsukahara, S. Yachi, H. Takeuchi, R. Takabe, W. Du, M. Baba, Y. Li, K. Toko, N. Usami, and T. Suemasu, Appl. Phys. Lett. **108**, 152101 (2016).
[18] D. K. Schroder and D. L. Meier, IEEE Trans. Electron Devices **31**, 637 (1984).
[19] S. Y. Lee, H. Choi, H. Li, K. Ji, S. Nam, J. Choi, S. W. Ahn, H. M. Lee, and B. Park, Sol. Energy Mater. Sol. Cells. **120**, 412 (2014).
[20] G. J. Bauhuis, P. Mulder, E. J. Haverkamp, J. C. C. M. Huijben, and J. J. Schermer, Sol. Energy Mater. Sol. Cells. **93**, 1488 (2009).
[21] K. Kuribayashi, H. Matsumoto, H. Uda, Y. Komatsu, A. Nakano, and S. Ikegami, Jpn. J. Appl. Phys., Part 1 **22**, 1828 (1983).
[22] K. Nishioka, T. Takamoto, T. Agui, M. Kaneiwa, Y. Uraoka, and T. Fuyuki, Sol. Energy Mater. Sol. Cells. **90**, 1308 (2006).
[23] M. A. Khan, M. S. Shur, and Q. Chen, Appl. Phys. Lett. **68**, 3022 (1996).
[24] L. L. Smith, R. F. Davis, M. J. Kim, R. W. Carpenter, and Y. Huang, J. Mater. Res. **12**, 2249 (1997).
[25] S. Okasaka, O. Kubo, D. Tamba, T. Ohashi, H. Tabata, and M. Katayama, Surf. Sci. **635**, 115 (2015).
[26] R. Takabe, K. Nakamura, M. Baba, W. Du, M. Ajmal Khan, K. Toko, M. Sasase, K. O. Hara, N. Usami, and T. Suemasu, Jpn. J. Appl. Phys. **53**, 04ER04 (2014).
[27] M. A. Khan, K. Nakamura, W. Du, K. Toko, N. Usami, and T. Suemasu, Appl. Phys. Lett. **104**, 252104 (2014).
[28] P. N. Vinod, J. Mater. Sci.: Mater. Electron. **22**, 1248 (2011).
[29] J. R. Sites and P. H. Mauk, Sol. Cells **27**, 411 (1989).